Electrostatics for Exploring Hydration Patterns of Molecules. 3. Uracil

Shridhar R. Gadre* and K. Babu

Department of Chemistry, University of Pune, Pune-411 007, India

Alistair P. Rendell

Supercomputer Facility, Australian National University, Canberra, ACT 0200, Australia

Received: March 28, 2000; In Final Form: July 21, 2000

A systematic investigation of the stepwise hydration of uracil has been carried out. The rich molecular electrostatic potential (MESP) topographical features of uracil provide clues on the probable water binding sites. The most noteworthy among these are the MESP minima due to carbonyl oxygens where the MESP value is negative as well as those over the uracil ring at which the MESP value is positive. Hydrated structures of uracil have been obtained employing an electrostatics-based model, EPIC (Electrostatic potential for Intermolecular Complexation) followed by ab initio optimization at the HF/6-31G(d,p) levels. Further geometry optimizations carried out at the HF/6-31+G(2d,p) and B3LYP/6-31+G(2d,p) levels, for smaller clusters, lead to trends in interaction energies which are in general agreement with those observed at the HF/6-31G-(d,p) level. These structures incorporate squares and cubes of water as the dominant building blocks. An analysis of the difference in interaction energies (ΔE_{rel}) of U...n(H_2O) and $(H_2O)_n$ clusters is seen to provide valuable information regarding hydration shells. This ΔE_{rel} stabilizes to −7 to −8 kcal mol^{-1} for $n > 8$ and this value of n may correspond to the number of water molecules that make up the first solvation shell of uracil, based on a criterion of the interaction energy.

Introduction

The process of hydration of molecules is of immense interest and significance to chemists and biologists alike. The role of hydration in chemistry has been well-recognized in phenomena such as ion solvation, rates of reactions, etc. As water permeates everywhere in the biosystem, hydrogen-bonded interactions of water also play a crucial role in most biological phenomena. With more sophisticated experimental tools and newer theoretical methods becoming available, detailed studies[1−10] of such interactions are increasing at a very rapid rate. Vibrational spectroscopy has long been a handy tool for experimentalists probing hydrogen-bonded systems. Conventionally, the red shift of the O−H stretching frequency is used as a tool for this purpose. Recent advances in this field have enabled more precise experimental investigations[1−5] on such systems, a brief review (far from a comprehensive one) of which is given below.

Several research groups have studied hydrogen bonding in phenol−water complexes. In 1996 Mikami and co-workers[1] investigated neutral and ionic clusters of phenol−$(H_2O)_n$, ($n \leq 4$) using advanced techniques in IR spectroscopy and pointed out the higher stability of structures involving water molecules that form a ring with the phenolic O−H. In 1998, Kleinermanns and co-workers[2a] observed the existence of "ice-like" cubical water clusters in phenol···n(H_2O) complexes, wherein the phenolic OH is either externally bonded to the water cube or forms part of a cubic cluster involving eight water molecules. They employed double-resonance vibronic spectroscopy to get a clear picture of the otherwise complex spectra. A further interesting conclusion was that complexes with less than eight waters still have cagelike cluster structures. Recently Chahinian et al.[3] exploited heteronuclear Overhauser spectroscopy to observe the hydrogen bonding in solvated uracil. They inferred that three water molecules (one in each of the amide group) form the first solvation shell of uracil. However, from the relaxation times of the coupled hetero-nuclei, one can only survey the number of hydrogen bonds on the neighboring atoms and no information about the total number of water molecules in the O=C−N−H site can be obtained. Hille[4] has experimentally investigated the molecular vibrations of hydrated uracil molecule in an argon matrix. Frequencies of these vibrations were found to be in fair agreement with the corresponding ab initio reaction field counterparts. Herschbach et al.[5] used mass spectroscopy to study the ionization potentials of free and hydrated nucleic acid bases (B) embedded in a supersonic molecular beam of moist argon. They obtained clusters as large as B···15(H_2O) and observed that the ionization potential decreases considerably with solvation. Benzene−water clusters have been explored by resonant ion-dip IR spectroscopy, and evidence for cubic water structures has been found.[5b]

On the theoretical front, it is now possible to perform calculations, of reasonable accuracy, on medium-sized aggregates of water with different molecules of interest. Semiempirical methods have been used in the past for this purpose, although their place has now largely been taken by molecular mechanics-type methods based on the use of well-parametrized force fields. In recent years due to the availability of greatly enhanced computing power, ab initio methods have also been applied to the hydration problem. All these approaches constitute discrete methods for studying solvation. On the other hand, self-consistent reaction field (SCRF)-type models incorporate the continuum effect due to solvent. However, they ignore the detailed molecule−solvent interactions. The difficulty with the explicit solvation method, especially at the ab initio level, is that one does not as yet have the computational power required

10.1021/jp001146n CCC: $19.00
Published on Web 09/06/2000

to study sufficiently large-sized aggregates so as to mimic the solvent medium. To overcome this shortcoming, there has been some effort directed toward the use of methods that combine the discrete and SCRF models.[6] In particular, Alemán has recently investigated this approach in an extensive study on the hydration of cytosine. His strategy[6a] combined discrete hydration studies of cytosine$\cdots H_2O$ complexes ($1 \leq n \leq 7$) with application of SCRF methods to obtain the free energy of solvation. It was found that this combined discrete/SCRF model provides a more reliable source for hydration studies as compared to purely continuum-based approaches. Such a methodology has earlier been employed by Alemán and Galembeck[6b] for studying solvation of the chromone molecule. However, both these studies considered mainly planar complexes and largely ignored three-dimensional growth of the aggregate. Leszczynski et al.[7] have carried out an elaborate study of solvent effects on the structure and properties of isocytosine−cytosine, guanine−cytosine, and adenine−uracil base pairs at the Hartree−Fock (HF) and correlated (second-order Møller Plesset-MP2) levels. They included the solvent effect by considering explicit water molecules, typically six to seven, coordinated to the base pair. The conclusion of their study is that there is not much deviation from planarity in the geometry of base pairs upon solvation, except for the Watson−Crick isocytosine−cytosine pair which shows considerable nonplanarity in the structure when six water molecules bind to it. The trends in the relative stability between different conformers are maintained, with a couple of exceptions, on solvation. However, they too have considered solvation due to water molecules only in the molecular plane and have not studied the effect due to water molecules approaching from above and below the plane of the base pairs. More recently, van Maurik et al.[8] have probed in detail the potential energy surface of uracil−water ($U\cdots H_2O$) complex using ab initio techniques at the MP2 level. In this study they used a very elaborate basis set and also corrected for basis set superposition error (BSSE). The interaction energies at MP2 level range from −6 to −9 kcal mol,$^{-1}$ with each of these local minima involving two hydrogen bonds between water and the uracil molecule. Such studies are potentially helpful for improving model potentials for $U\cdots H_2O$ interactions. Gordon and co-workers[9] have proposed an effective fragment potential model for studying weak intermolecular interaction. They have investigated explicit hydration of formamide and have found rings of four and five water molecules in the hydrated complex. Structure−property considerations have also been applied for studying solvation free energies (ΔG_{sol}). Recently, Politzer et al.[10] have obtained an equation for ΔG_{sol} in terms of surface molecular electrostatic properties for a number of solute molecules. A good correlation with the experimentally determined solvation energies was obtained.

It is generally agreed that electrostatics plays a dominant role in hydration processes. The utility of topography mapping of the molecular electrostatic potential (MESP) has recently been highlighted[11] for studying these processes. In particular, a model, viz. electrostatic potential for intermolecular complexation (EPIC)[12] employing MESP and other derived quantities as basic inputs, has been found to be quite successful for this purpose. The purpose of the present work is to undertake a systematic investigation of the clusters obtained by the explicit hydration of uracil with electrostatic guidelines as exemplified by $U\cdots(H_2O)_n$ clusters. No attempt is made to mimic aqueous solution of uracil. Though hydration has been studied widely by several research workers, many of these studies (as noted above) have focused on clusters in which water molecules bind only to the primary binding sites on the host molecule, with additional water molecules forming hydrogen bonded networks to these primary waters. Our aim in this study is to explore the hydrated structures wherein the host molecule can also be an active part of the networked cluster.

Methods

Molecular Electrostatic Potential (MESP) and Its Topography. The electrostatic potential, $V(\mathbf{r})$ at a point $\mathbf{r}$ generated by a molecule is given by

$$V(\mathbf{r}) = \sum_{A}^{N} \frac{Z_A}{|\mathbf{r} - \mathbf{R}_A|} - \int \frac{\rho(\mathbf{r}')d^3r'}{|\mathbf{r} - \mathbf{r}'|}$$

where the first term denotes the contribution due to nuclei of charges $\{Z_A\}$ located at $\{\mathbf{R}_A\}$ and the second term arises due to the continuous electronic charge density distribution, $\rho(\mathbf{r})$. Points where the first derivative of MESP, with respect to the Cartesian axes, becomes zero viz. $\nabla V(\mathbf{r}) = 0$ are called the critical points (CP). These CPs can be characterized based on the number and nature of the nonzero eigenvalues of the second derivative matrix A, where $A_{ij} = (\partial^2 f/\partial x_i \partial x_j)$, evaluated at the CP. If one or more of the eigenvalues is/are zero, it represents a degenerate CP. With R representing the rank of the second derivative matrix and σ the sum of the signs of the nonzero eigenvalues, the CP is labeled as (R, σ). Obviously, the rank of a nondegenerate CP of molecular scalar fields such as the MESP is always three. Hence, such an MESP CP can be of type (3, +3), viz. a minimum, that typically represents electron localization, (3, −3) a maximum (for molecules) or (3, −1) and (3, +1) saddles that bridge either two minima or two maxima. Further, it has been rigorously proven by Gadre et al.[13] that nonnuclear maxima do not exist within the scalar field of the MESP. Each type of MESP CP has its own chemical significance. For example, lone pairs of electrons as well as C=C π bonds generally show up as negative valued MESP minima, viz. (3, +3) CPs. Every pair of bonded atoms is generally characterized by a positive-valued (3, −1) type bond saddle. Several detailed investigations of MESP topography have been reported by Gadre and co-workers[14] during the last eight years for a variety of anionic and molecular species. Earlier, Bader[15] pioneered such investigations on the topography of molecular electron densities. By locating MESP CPs, one can precisely identify the electrophilic and nucleophilic binding sites on a molecule. In the present study, the MESP and corresponding CPs of uracil were computed using the program UNIPROP.[16a]

Electrostatic Potential for Intermolecular Complexation (EPIC). An electrostatic-based model (EPIC) capable of generating reasonable geometries and interaction energies of weakly bonded complexes has been developed by Gadre et al.[14,16b] In this program, the electrostatic interaction energy of a weakly bound molecular cluster is estimated as

$$E_{EPIC} = 1/2 \sum_{A}^{N} \sum_{\substack{B \neq A \\ i \in B}}^{N} V_{A,i} q_{B,i}$$

where, $V_{A,i}$ is the MESP at atomic centers {i} on molecule B due to all the molecules in the complex sans B, $q_{B,i}$ are the MESP-derived point charges obtained using the program GRID.[16c] This interaction energy is then minimized by optimizing the geometry while adhering to the rigid molecule approximation, i.e., the internal geometry of each molecule is held fixed while the molecules are rolled over one another. The van

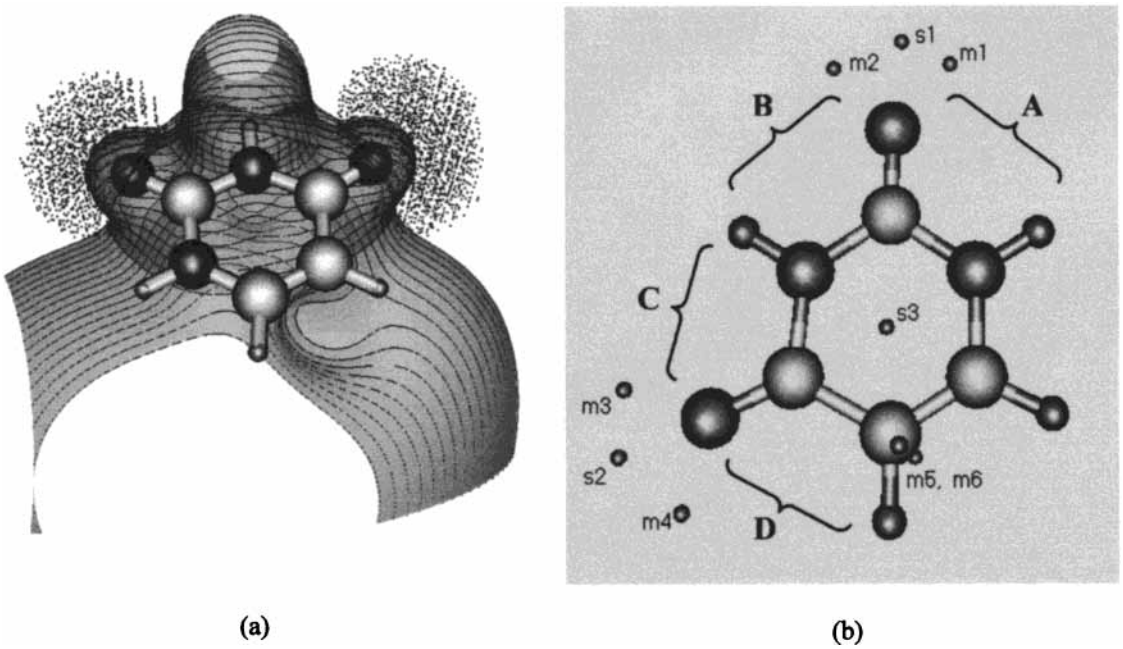

Figure 1. (a) Isosurface and contours of MESP value 6.28 kcal mol^{-1} and fuzzy surface of MESP value -31.38 kcal mol^{-1}; (b) MESP topography of uracil. The points m1 to m6 denote MESP minima and s1 to s3 denote (3, +1) saddles. The corresponding MESP values, in kcal mol^{-1}, are -50.20 (m1), -52.71 (m2), -54.59 (m3), -57.73 (m4), +0.31 (m5 and m6), -49.95 (s1), -55.82 (s2), +160.33 (s3). A, B, C, and D indicate the primary binding sites in uracil molecule.

der Waals surfaces are defined to avoid the molecules approaching too close (getting into coalescing distance). Standard optimization algorithms such as cyclic relaxation, simulated annealing, and genetic algorithm are used for this purpose. This program has been tested on a variety of systems. The interaction energies and geometries of the complex provided by EPIC are generally found to be comparable with their ab initio counterparts.

Ab Initio Calculations. All the ab initio gas-phase calculations have been carried out at the HF/6-31G(d,p) level of theory using the GAUSSIAN[17] suite of programs and GAMESS.[18] Higher level calculations at HF/6-31+G(2d,p) and DFT B3LYP/6-31+G(2d,p) have also been done for clusters of smaller size with a view to assess the basis-set and correlation effects. The graphics visualization package UNIVIS-2000[16d] has been used to produce all the figures.

Results and Discussion

The uracil molecule (U) was optimized at the HF/6-31G(d,p) level, and subsequently the vibrational frequencies were evaluated. From this optimized geometry and wave function, the MESP topography was mapped using the program UNIPROP.[16a] Figure 1a depicts the fuzzy isosurface corresponding to the MESP value of -31.38 kcal mol^{-1} and a rendered isosurface with the MESP value of 6.28 kcal mol^{-1} superposed with the respective contours of identical value. In Figure 1a, a cross-section of the latter isosurface and the respective contours are shown so as to bring out a three-dimensional view. This figure reveals an interesting feature: the MESP over the entire ring region is positive. With the complementary lock-and-key features of MESP in mind, we may hence expect that a water molecule positioned over the uracil ring to orient in such a way that the corresponding "rabbit ears" (i.e., the negative valued oxygen lone pair minima) point toward the uracil ring. This is a unique feature indeed since for the benzene molecule exactly the reverse is seen, i.e., the six negative-valued minima over the ring lead to O$-$H$\cdots\pi$ interactions where the H of water binds with the ring.

The MESP topographical features of uracil are shown in Figure 1b with the corresponding MESP values reported in the caption. Each of the carbonyl oxygen atoms exhibits two negative-valued minima (m1 through m4) with a connecting (s1 and s2) saddle. The occurrence of positive-valued (6.28 kcal mol^{-1}) minima (m5 and m6) corresponding to the C$=$C bond is also a very distinct feature of the molecule. It may be noted that the ethylene double bond normally[14] shows its signature as a pair of negative valued MESP minima. Conspicuous by their absence are the negative-valued minima over the nitrogen atoms. Uracil is thus seen to possess three strong primary binding sites A, B, and C where water can form two hydrogen bonds with the amide group in the ring, while the fourth site, D can form only one hydrogen bond with water.

Geometries of U$\cdots$H$_2$O have been generated making use of the topographical characteristics discussed above, while maintaining complementarity between the MESP features of uracil and water. The ab initio optimized geometries of individual uracil and water molecules are used for this purpose. These two have then been docked with EPIC and the geometries provided by EPIC were subjected to ab initio optimization.

Figure 2 depicts the geometries of EPIC-optimized U$\cdots n$H$_2$O for a few selected structures corresponding to $n = 1$, 2, and 4. Four geometries for U$\cdots$H$_2$O complex are displayed as U1A, U1B, U1C, and U1D, respectively, corresponding to four distinct sites in U as shown in Figure 1b. These geometries were further subjected to ab initio optimization. However, the resulting ab inito geometries are very similar to those in Figure 2 and hence are not displayed separately. The corresponding energy values are displayed in Table 1. It may be seen that the trends shown by EPIC interaction energies are generally in agreement with the ab initio results. The geometries obtained from EPIC are generally seen to provide good initial guesses for HF optimization with a substantial reduction in computational time. These

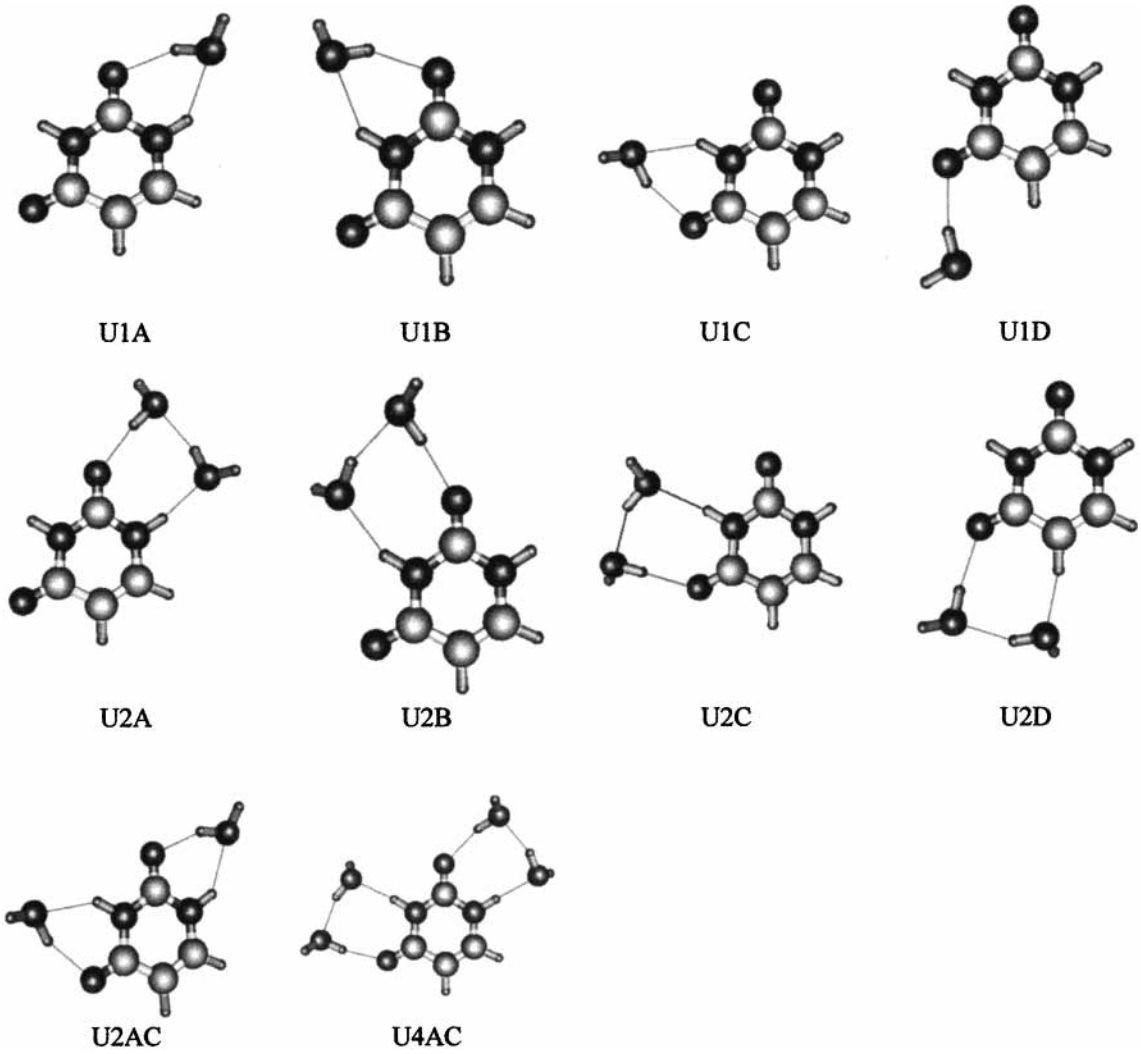

Figure 2. EPIC-optimized geometries of U···H_2O, U···$2H_2O$, and U···$4H_2O$. See text for details and Table 1 for the corresponding interaction energies.

TABLE 1: Interaction energies (in kcal mol^{-1}) of EPIC and ab Initio Optimized U···nH_2O (n = 1, 2, 4, and 6) Complexes[a]

struct.	ΔE_{EPIC}	ΔE_{HF}/ 6-31G(d,p) (A)	ΔE_{HF}/ 6-31+G(2d,p) (B)	ΔE_{DFT}/B3LYP 6-31+G(2d,p) (C)	(B/A)	(C/A)
U1A	−10.81	−10.63	−8.17	−9.93	0.77	0.93
U1B	−7.46	−8.61	−6.24	−7.78	0.72	0.90
U1C	−9.34	−9.00	−6.52	−8.47	0.72	0.94
U1D	−6.18	−6.92	−5.57	−6.67	0.80	0.96
U2A	−21.00	−22.19	−17.37	−21.52	0.78	0.97
U2B	−14.74	−18.93	−14.40	−18.24	0.76	0.92
U2C	−16.27	−19.36	−14.80	−19.02	0.76	0.98
U2D	−20.85	−16.55	−12.71	−15.69	0.76	0.94
U2AC	−20.38	−19.82	−14.88	−18.60	0.75	0.94
U4A	−34.55	−41.42	−31.62	−39.48	0.76	0.95
U4AC	−37.27	−41.84	−32.37	−40.79	0.77	0.97
U6A1	−49.80	−62.69	−46.32	−58.11	0.73	0.93
U6A2	-	−61.70	−46.22	−58.38	0.75	0.94
U6P	-	−57.51	−43.52	−54.86	0.75	0.95

[a] See Figure 2 and text for details.

trends in the energies of these structures are similar to those reported by van Mourik et al.[8] in their elaborate MP2-level calculations.

A similar exercise has been undertaken for a few select geometries of U···$2H_2O$. These structures, denoted as U2A−U2AC are shown in Figure 2. It is seen from the energy values that U2A is the lowest energy structure for these dihydrated species, a trend also borne out at the HF level. The other structures are also generally of comparable energies with the HF energy values lying between −16 to −22 kcal mol^{-1}. Many possible structures of U···$4H_2O$ have been explored by EPIC as well as by ab initio methods. However, due to the lack of space, only the lowest energy structures are reported here. Similarly, only three ab initio optimized structures of U···$6H_2O$ are displayed in Figure 3 with the interaction energies at the HF level ranging from −57 to −63 kcal mol.$^{-1}$ This range is in accord with the ballpark figure of −10 kcal mol^{-1} per water obtained for the structures mentioned earlier as well as from the studies on hydration of formamide.[22b] It may be noticed from Figure 3 that square and cubic patterns indeed emerge as stable structures, as has been pointed out in the earlier studies on similar moieties.[2a]

With this experience in hand, it was felt that carrying out further EPIC calculations was not necessary for the higher hydrated structures. Instead, subsequent studies on hydration were carried out by employing the basic patterns revealed by the above-mentioned ab initio optimized structures. Cutting of the water rings and cages from these structures to obtain templates and patching these templates to the host molecule provides good guess geometry for the higher aggregates. In particular, the square and cubic patterns have been tried for geometries of U···nH_2O corresponding to n = 10, 12, and 15. The respective ab initio optimized structures are denoted as

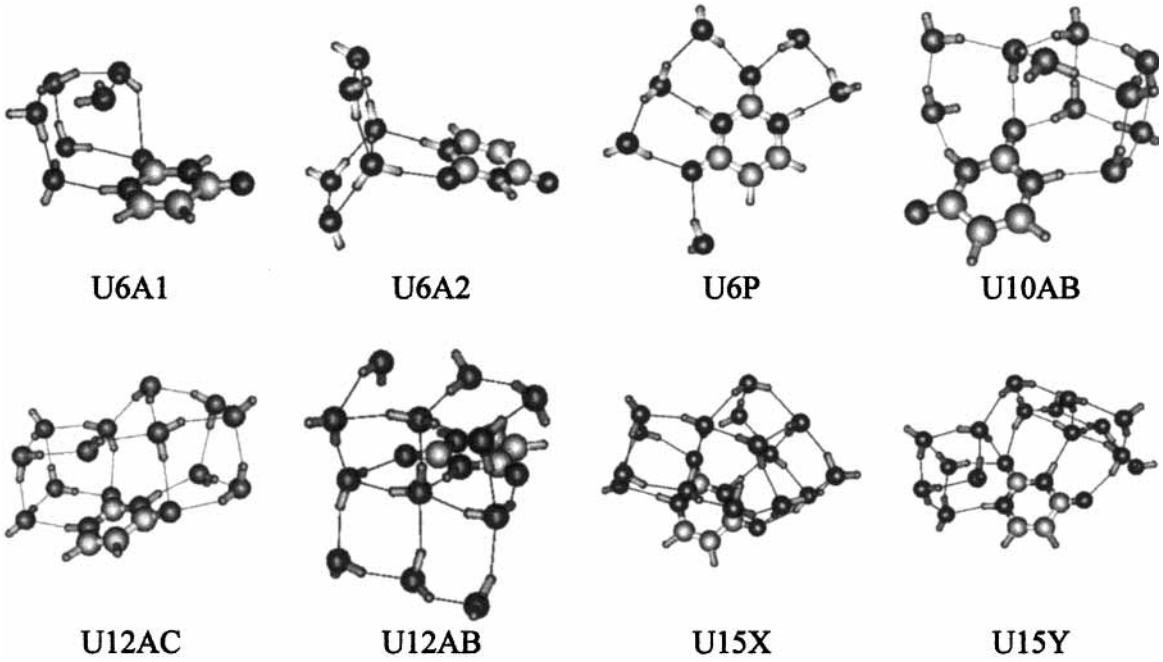

Figure 3. The ab initio [HF/6-31G(d,p)] optimized geometries of U...nH_2O, $n = 6$, 10, 12 and 15. See text for details and Tables 1 and 2 for interaction energies.

TABLE 2: Interaction Energies (in kcal mol^{-1}) of ab Initio Optimized (at HF/6-31G(d,p) Level) U$\cdots n$$H_2O$ ($n = 8$, 10, 12, and 15) Complexes[a]

structure	ΔE_{HF}
U8A	−86.00
U10A	−103.93
U10AB	−105.50
U12AB	−116.40
U12AC	−129.07
U15X	−162.89
U15Y	−151.76

[a] See Figure 3 and text for details.

U10A, U10AB, U12AB, U12AC, U15X, and U15Y, respectively, in Figure 3 and Table 2.

It may be seen from the energies reported in Table 1 that the planar structure of U$\cdots$6H_2O is the least favored hexacoordinated structure. This is noteworthy since Chahinian et al.[3] in their magnetic resonance study of uracil did not consider this possibility. Instead they concluded that the solvation shell in uracil was made up of just three water molecules binding, one each, to the sites denoted here as A, B, and C. Similarly Alemán[6] and Leczszynski et al.[7] in their study of the solvation of nucleic acid base pairs considered water molecules to be binding in the plane of the host molecule. Clearly the three-dimensional hydrated structures reported in Figure 3 indicate that further studies on this aspect are warranted.

The sample structure of U$\cdots$10H_2O (U10AB) displayed in Figure 3 shows a predominance of five-membered rings. Going further to U$\cdots$12H_2O, one finds a combination of cubic and square patterns, two such typical structures (U12AB and U12AC) are shown in Figure 3. Structure U12AC has been obtained by replicating the water cube at site A in U6A1 and patching it at site C followed by flipping of the hydrogen atoms so as to get a favorable interaction between the two cubical patterns. The structure U12AB also reveals the square patterns. Two cubes can be seen adjacent to each other at sites A and B, while water molecules on the other side of the plane form squares at the same sites. Structure U12AC shows higher stabilization than U12AB though it has two hydrogen bonds less than U12AB. This is due to two facts. First, the structure U12AC has two oxygen atoms, one in each of the water cubes, which point toward the positive MESP region of the uracil ring, as pointed out earlier (cf. Figure 1). On the other hand, the structure U12AB has only one such interaction and even in that case the oxygen is not properly oriented, as it is the bridging atom between the two cubes. Second, the cubical patterns in U12AB are greatly distorted compared to those in U12AC. Step-by-step increment in the number of water molecules leads to structures U15X and U15Y. The presence of four distorted cubic structural patterns can be seen in U15X, while U15Y contains one cube at site C and partly built cubes at sites A and B on both sides of the molecular plane. It should be noted again that in U15X, the oxygen atom of the water molecule located over the central region of the ring has its oxygen pointing toward the ring.

For many of the structures reported here frequency evaluations have been performed at the HF level in order to verify that we have indeed located local minima on the potential energy surface. Typically such a vibrational frequency analysis shows several frequencies of magnitude less than 100 cm^{-1} corresponding to modes which are spread over large hydrogen-bonded networks. This indicates a very flat potential energy surface, which when coupled with the huge number of arrangements of water molecules around uracil makes it very difficult to ensure that the energies reported in Tables 1 and 2 represent global minima. In this respect, sufficient search has been made for structures with $1 \leq n \leq 10$ for which we are fairly confident that we have located the global minima. However, a more thorough search may be needed for the $n = 12$ and 15 cases.

The insights offered by the electrostatic considerations as well as by systematic building-up of hydrated clusters using basic patterns such as squares, pentagons, and cubes are found to be useful in these quantum-chemical calculations. As a rule of thumb, an interaction energy of approximately (ΔE_{HF}) −10 kcal mol^{-1} per H_2O seems to be valid for the hydration of uracil. A look at the Koopmans' ionization potential (IP) of free uracil and a few hydrated structures ($1 \leq n \leq 10$) shows that the IP does, generally, decrease upon successive hydration: the IP

values steadily dropping from 10.0 to 9.5 eV. Such behavior has been observed earlier by Herschbach et al.[5a] through their IP measurements. However, since the reported structures U···12H_2O and U···15 H_2O may not represent global minima, we have not included these structures in this analysis of IPs.

Are these calculations at HF/6-31G(d,p) level reliable? Our experience[12,22] indicates that this level of theory engenders reasonably good estimates of interaction energies. This level and basis are also known to be quite reliable[14] for obtaining the topographical features of the MESP. To assess the role of correlation we have performed a few density functional theory based calculations at B3LYP level.[17] This is due to the fact that optimizations at the MP2 or coupled-cluster level level are computationally very expensive. For test calculations performed on U···$n$$H_2O$, with $n = 10$ and 12, the B3LYP binding energies (ΔE_{DFT}) turn out to be -216.28 and -265.32 kcal mol^{-1}, respectively. As expected, these interaction energies are numerically larger than the HF results due to the incorporation of electron correlation effects. However, also as expected, these values are excessively large which is an artifact of the shorter hydrogen bond lengths predicted by the DFT: the typical O···H bond length being 1.7 Å as against 2.0 Å for their HF counterparts.

With a view to further assess the basis-set and correlation effects, geometry optimizations for U···$n$$H_2O$, $1 \leq n \leq 6$, clusters at the HF/6-31+G(2d,p) level and with DFT at B3LYP/6-31+G(2d,p) level have been carried out. The interaction energies at these higher levels, reported in Table 1, also fall in line with the ΔE trends at HF/6-31G(d,p). Surprisingly, even the ΔE_{DFT} trends match exactly with those of ΔE_{HF}, and in fact these ΔE_{HF} and ΔE_{DFT} trends at 6-31+G(2d,p) basis scale approximately linearly with ΔE_{HF}/6-31G(d,p), the corresponding scaling factors being given in the last two columns of Table 1. It is also noteworthy that the interaction energies and even the geometrical parameters at B3LYP/6-31+G(2d,p) are much closer to the corresponding values at HF/6-31G(d,p). This is due to two opposing factors: (a) the exchange correlation in DFT decreases the contact distances between the interacting molecules and increases the normal bond distances, while overestimating the interaction energy; (b) improving the basis from 6-31G(d,p) to 6-31+G(2d,p) brings down the interaction also producing reverse effects in the weak and covalent bond distances. These two converse factors lead to the interaction energies and geometrical parameters at HF/6-31G(d,p) and B3LYP/6-31+G(2d,p) levels being strikingly closer.

One may also wonder about the basis-set superposition error (BSSE). To assess BSSE, the counterpoise method of Boys and Bernardi[23] was applied to two clusters, viz. U6A1 and U10A. While calculating the monomer energies their respective geometries were restored to the HF/6-31G(d,p) ones applying appropriately defined Z-matrix. Hence our BSSE corrections are larger than those normally reported in the literature (without restoring the monomers to their respective geometries). The BSSE-corrected (uncorrected) interaction energies for these two clusters are -50.63 (-62.68) and -83.58 (-103.93) kcal mol^{-1} respectively. A typical scale factor of $\sim$0.8 hence seems to be applicable for this purpose. With this observation, we have not carried out BSSE corrections for the other clusters.

In the above discussion, we have emphasized the interaction energy of the U···$n$$H_2O$ structures. It is instructive to compare this with the interaction energy of $(H_2O)_n$ clusters[24] for $2 \leq n \leq 15$. Due to the large size of the systems involved, only HF/6-31G(d,p) level computations have been performed. The difference between these two interaction energies is given by $\Delta E_{rel} = \Delta E_{U\cdots n(H_2O)} - \Delta E_{n(H_2O)} = E_{U\cdots nH_2O} - E_U - E_{n(H_2O)}$. We have analyzed only a few values of n, and report results in Table 3. The ΔE_{rel} values for $n = 5$ and 6 are numerically quite large viz. -13.15 and -13.16 kcal mol^{-1}, respectively. However, they show a general downward trend from $n = 10$ onward, the corresponding ΔE_{rel} values being in the range of -9 to -7 kcal mol^{-1}. It is clear that ΔE_{rel} represents the net gain in stabilization due to optimization of n water molecules (originally from $(H_2O)_n$ cluster) in the presence of the uracil moiety. This drop in the magnitude of ΔE_{rel} on going from $n = 6$ to $n = 10$ may be a pointer to the shell structure in solvation. On going further from $n = 10$ case, it appears that H_2O···H_2O interactions take over, resulting in a leveling of the ΔE_{rel} value. Notice that the incremental interaction energy value is -33.0 kcal mol^{-1} for $(H_2O)_{15}$ cluster as compared to -25.1 kcal mol^{-1} for $(H_2O)_{12}$. A similar exercise carried out for U···15(H_2O) and U···12(H_2O), using the values from the third column of Table 3 gives an energy enhancement of -33.8 kcal mol^{-1} and -23.6 kcal mol^{-1}, respectively. These two incremental energies are indeed very close to each other indicating that for hydration of uracil beyond 12H_2O molecules, it is predominantly water−water interactions. Due to the approximately linear scaling of the energies reported in Table 1 (vis-à-vis the basis-set/level of theory) the above trends are expected also to hold for enhanced basis-set/theory level. Similar studies on the hydration of other substrates would provide valuable clues on the solution behavior. These studies are currently underway in our laboratory.

TABLE 3: Interaction Energies (in kcal mol^{-1}) of ab Initio Optimized (at HF/6-31G(d,p) Level) U···$n$$H_2O$ and $(H_2O)_n$ Complexes ($n = 5$, 6, 8, 10, 12, and 15)[a] along with the Difference between Them

n	$\Delta E_{n(H_2O)}$	$\Delta E_{U\cdots n(H_2O)}$	ΔE_{rel}
5	−37.75	−50.9	−13.15
6	−49.57	−62.68	−13.11
8	−76.04	−86.00	−9.96
10	−96.77	−105.50	−8.74
12	−121.88	−129.07	−7.19
15	−154.88	−162.89	−8.01

[a] See text for details.

Concluding Remarks

In the earlier articles[22] of this series, the utility of electrostatic considerations for studying the hydration of molecules has been demonstrated. In particular, the MESP CPs are seen to serve as a harbinger to the interacting water molecules. The EPIC model exploits these electrostatic features for obtaining reasonably good estimates of interaction energies as well as the structure of hydrated species. In the case of the uracil molecule, the first few water molecules are bonded to the most negative MESP minima corresponding to the carbonyl oxygen lone pairs. It is seen that the EPIC model indeed brings out correct trends in interaction energies of the hydrated species. The corresponding geometries serve as excellent starting points for the subsequent HF level calculations. A unique feature of the MESP topography of uracil is the depletion of electrons from the region above the ring. It may qualitatively be predicted that a water molecule placed above/below the uracil ring will have its oxygen pointing toward the ring. Such a feature is indeed revealed by the structures of U···n(H_2O) species for $n \geq 6$, shown in Figure 3. Yet another interesting feature is the occurrence of some standard building blocks such as the squares, pentagons, and cubes, in the structure of hydrated uracil moiety. This is in conformity with the findings on hydration of phenol,[2] although

the earlier studies on DNA-bases have perhaps not explored these patterns. Thus the occurrence of square- and cubelike patterns does not seem to be restricted to aromatic molecules as thought earlier.[2]

The calculations reported in the present study have been carried out at the HF/6-31G(d,p) level which is known to be reasonably good for capturing the essential MESP topographical features as well as interaction energies. This fact has also been confirmed by performing calculations with larger basis sets and with DFT methods for clusters with six or less water molecules. Improving the basis or inclusion of exchange correlation through DFT did not bring about any change in the inferences obtained at the HF/6-31F(d,p) level.

Due to the shallow nature of the potential energy surfaces of such systems, it may be difficult to ensure attainment of the global minimum. In U···n(H_2O) clusters $1 \leq n \leq 10$, however, sufficient care has been taken to ensure that we are reasonably close to the global minimum. BSSE correction seems to generally scale down the respective interaction energies by a constant factor ($\sim$0.8).

With the analysis of the interaction energies of $(H_2O)_n$ and U...n(H_2O) clusters presented in Table 3, it is clear that U acts as a structure maker. The number of water molecules favorably bound to U from an energetic point of view seems to be about 6. Going further from $n = 6$, a general downward trend is seen in the ΔE_{rel} values, leveling out at about -8 kcal mol^{-1} for $n = 15$. The interaction energy of adding three water molecules to U···12(H_2O) resembles the corresponding energy increments for adding three water molecules to $(H_2O)_{12}$ clusters. Hence it seems that water−water interactions takes over the U···H_2O interaction beyond $n = 12$.

In summary, the present electrostatics-guided hydration study of uracil is able to bring out the explicit hydration patterns as well as the shell structure quite well. It should be emphasized again that this work employs an approach based on clusters: the hydration patterns in liquid water could be different. It is hoped that such an approach, on extensive testing for more molecules, would bridge the gap between quantum-chemical studies and Monte Carlo/molecular dynamics investigations of solutions.

Acknowledgment. Financial support from the Council of Scientific and Industrial Research (CSIR), New Delhi, is gratefully acknowledged. We are thankful to Drs. W. Roth and B. Hartke for providing us with the structures and energies of some $(H_2O)_n$ clusters. The ab initio computations reported in this work have been carried out at the Centre for Development of Advanced Computing (C-DAC), Pune, India, and the Supercomputing Facility of the Australian National University, Canberra. We are thankful to them for providing us with computational facilities. A.P.R. gratefully acknowledges the support of SUN Microsystems. The authors thank Dr. Ajay C. Limaye for his assistance in producing figures employing UNIVIS-2000 package.

References and Notes

(1) Ebata, T.; Fujii, A.; Mikami, N. *Intern. J. Mass Spectrom. Ion Processes* **1996**, *159*, 111.

(2) (a) Jacoby, Ch.; Roth, W.; Schmitt, M.; Janzen, Ch.; Spangenberg, D.; Kleinermanns, K. *J. Phys. Chem.* **1998**, *A102*, 4471. (b) Roth, W.; Schmitt, M.; Jacoby, Ch.; Spangenberg, D.; Janzen, Ch.; Kleinermanns, K. *Chem. Phys.* **1998**, *239*, 1. (c) Janzen, Ch.; Spangenberg, D.; Roth, W.; Kleinermanns, K. *J. Chem. Phys.* **1999**, *110*, 9898.

(3) Chahinian, M.; Seba, H. B.; Arician, B. *Chem. Phys. Lett.* **1998**, *285*, 337.

(4) Hille, R. *J. Phys. Chem.* **1997**, *B101*, 10923.

(5) Kim, S. K.; Lee, W.; Herschbach, D. R. *J. Phys. Chem.* **1996**, *100*, 7933. (b) For studies of benzene−water octamers by spectroscopic methods, see Gruenloh, C. J.; Carney, J. R.; Hagemeister, F. C.; Arrington, C. A.; Zwier, T. S.; Fredericks, S. Y.; Woods, J. T.; Jordan, K. D. *J. Chem. Phys.* **1998**, *109*, 6601 and references therein.

(6) Alemán, C. *Chem. Phys.* **1999**, *244*, 151. (b) Alemán, C.; Galembeck, S. E. *Chem. Phys.* **1998**, *232*, 151.

(7) Zhanpeisov, N. U.; Leszczynski, J. *J. Mol. Struct. (THEOCHEM)* **1999**, *487*, 107. Zhanpeisov, N. U.; Leszczynski, J. *J. Phys. Chem.* **1998**, *A102*, 10374. Zhanpeisov, N. U.; Leszczynski, J. *J. Phys. Chem.* **1998**, *B102*, 9109. Zhanpeisov, N. U.; Leszczynski, J. *J. Phys. Chem.* **1998**, *A102*, 6167. Zhanpeisov, N. U.; Leszczynski, J. *Int. J. Quantum Chem.* **1998**, *69*, 37.

(8) van Mourik, T.; Price, S. L.; Clary, D. C. *J. Phys. Chem.* **1999**, *A103*, 1611.

(9) Chang, W.; Gordon, M. S. *J. Chem. Phys.* **1996**, *105*, 11081.

(10) See, for a recent discussion of solvation free energy obtained from surface molecular electrostatic potentials, Murray, J. S.; Abu-Awwad, F.; Politzer, P. *J. Phys. Chem.* **1999**, *A103*, 1853 and references therein.

(11) See, for comprehesive reviews, *Chemical Applications of Atomic and Molecular Electrostatic Potentials*; Politzer, P., Truhlar, D. G., Eds.; Plenum: New York, 1982. *Molecular Electrostatic Potentials: Concepts and Applications*; Murray, J. S., Sen, K. D., Eds.; Elsevier: Amsterdam, 1996.

(12) See, for example, Gadre, S. R.; Bhadane, P. K.; Pundlik, S. S.; Pingale, S. S. in *Molecular Electrostatic Potentials: Concepts and Applications*; Murray, J. S., Sen, K. D., Eds.; Elsevier: Amsterdam, 1996.

(13) Gadre; S. R.; Pathak, R. K. *Proc. Ind. Acad. Sci. (Chem. Sci.)* **1990**, *102*, 189. Pathak, R. K. *J. Chem. Phys.* **1990**, *93*, 1770.

(14) Gadre, S. R.; Shrivastava, I. H. *J. Chem. Phys.* **1991**, *94*, 4384. Gadre, S. R.; Kulkarni, S. A.; Shrivastava, I. H. *J. Chem. Phys.* **1992**, *96*, 5253. Gadre, S. R.; Kulkarni, S. A.; Suresh, C. H.; Shrivastava, I. H. *Chem. Phys. Lett.* **1995**, *239*, 273. Pingale, S. S.; Gadre, S. R.; Bartolotti, L. J. *J. Phys. Chem.* **1998**, *A102*, 9987.

(15) Bader, R. F. W. *Chem. Rev.* **1991**, *91*, 893. Bader, R. F. W.; Nguyen-Dang, J. T. *Advanced Quantum Chemistry;* Löwdin, P.-O., Ed.; Academic: New York, 1981; Vol. 14, p 63. Bader, R. F. W. *Atoms in Molecules: a Quantum Theory*; Oxford University Press: Oxford, 1990.

(16) The package *UNIPROP* was developed by S. R. Gadre and coworkers, Department of Chemistry, University of Pune, 411 007, India. (b) Pundlik, S. S. *Development of an electrostatic model for weak intermolecular complexeaton (EPIC)*; Ph.D. Thesis, University of Pune, Pune, India, 1998. (c) Chipot, C. GRID: *Fortran program performing charge fitting to molecular electrostatic potentials or fields.* Laboratoire de Chimie Théorique, Unité de Recherche Associée au CNRS no. 510, Université de Nancy I, BP 239, 54506 Vandceuvre-lès-Nancy Cedex, France, 1992. (d) A new package viz. UNIVIS-2000 (α-release) being developed by S. R. Gadre and A. C. Limaye is employed for visualization purposes in the present work. For the older DOS-based version of UNIVIS, see Limaye, A. C.; Inamdar, P. V.; Dattawadkar, S. M.; Gadre, S. R. *J. Mol. Graph.* **1996**, *14*, 19.

(17) Frisch, M. J.; Trucks, G. W.; Schlegel, H. B.; Gill, P. M. W.; Johnson, B. G.; Robb, M. A.; Cheeseman, J. R.; Keith, T.; Petersson, G. A.; Montgomery, J. A.; Raghavachari, K.; Al-Laham, M. A.; Zakrzewski, V. G.; Ortiz, J. V.; Foresman, J. B.; Peng, C. Y.; Ayala, P. Y.; Chen, W.; Wong, M. W.; Andres, J. L.; Replogle, E. S.; Gomperts, R.; Martin, R. L.; Fox, D. J.; Binkley, J. S.; Defrees, D. J.; Baker, J.; Stewart, J. P.; Head-Gordon, M.; Gonzalez, C.; Pople, J. A. *Gaussian 94*; Gaussian, Inc.: Pittsburgh, PA, 1995.

(18) The package GAMESS, Schmidt, M. W.; Baldridge, K. K.; Boatz, J. A.; Elbert, S. T.; Gordon, M. S.; Jensen, J. H.; Koseki, S.; Matsunaga, N.; Nguyen, K. A.; Su, S. J.; Windus, T. L. together with Dupuis, M.; Montgomery, J. A. *J. Comput. Chem.* **1993**, *14*, 1347. Parallel version of the GAMESS running on a large parallel (a cluster of 40 SUN Ultra 450 machines) computer, PARAM, developed by the Centre for Development of Advanced Computing (C-DAC), has been used in the present study.

(19) Dolgounitcheva, O.; Zakrzewski, V. G.; Ortiz, J. V. *J. Phys. Chem.* **1999**, *A103*, 7912.

(20) Pingale, S. S.; Gadre, S. R.; Bartolotti, L. J. *J. Phys. Chem.* **1998**, *A102*, 9987. (b) Gadre, S. R.; Kulkarni, A. D. *Ind. J. Chem.* **2000**, *39A*, 50 [papers 1 and 2 of this series, respectively].

(21) Boys, S. F.; Bernardi, F. *Mol. Phys.* **1970**, *19*, 553.

(22) The $(H_2O)_n$ water cluster energies and geometries were taken from Wales, D. J.; Hodges, M. P. *Chem. Phys. Lett.* **1998**, *286*, 65. See also Khan, A. *J. Phys. Chem.* **1995**, *99*, 12450. Hartke, B.; Schuetz, M.; Werner, H.-J. *Chem. Phys.* **1998**, *239*, 561. cf. the following websites: http://brian.ch.cam.ac.uk/~wales/CCD/TIP4P-water.html, http://www-public.rz.uni-duesseldorf.de/~rothw/gauss/abinitio.html